Kinetics of Precursor Labeling in Stable Isotope Labeling in Cell Cultures (SILAC) Experiments

ARTICLE *in* ANALYTICAL CHEMISTRY · OCTOBER 2014

Impact Factor: 5.64 · DOI: 10.1021/ac503067a · Source: PubMed

analytical chemistry

Article

pubs.acs.org/ac

Kinetics of Precursor Labeling in Stable Isotope Labeling in Cell Cultures (SILAC) Experiments

Tian Zhang,[†] John C. Price,[§] Eslam Nouri-Nigjeh,[‡] Jun Li,[‡] Marc K. Hellerstein,[∥,⊥] Jun Qu,[‡] and Sina Ghaemmaghami*,[†]

[†]Department of Biology, University of Rochester, Rochester, New York 14627, United States

[‡]Department of Pharmaceutical Sciences, University at Buffalo, Buffalo, New York 14215, United States

[§]Department of Chemistry and Biochemistry, Brigham Young University, Provo, Utah 84602, United States

[∥]Department of Nutritional Science and Toxicology, University of California, Berkeley, Berkeley, California 94720, United States

[⊥]KineMed, Inc., Emeryville, California 94608, United States

Supporting Information

ABSTRACT: Recent advances in mass spectrometry have enabled proteome-wide analyses of cellular protein turnover. These studies have been greatly propelled by the development of stable isotope labeling in cell cultures (SILAC), a set of standardized protocols, reagents aimed at quantifying the incorporation of $^{15}N/^{13}C$ labeled amino acids into proteins. In dynamic SILAC experiments, the degree of isotope incorporation in proteins is measured over time and used to determine turnover kinetics. However, the kinetics of isotope incorporation in proteins can potentially be influenced not only by their intracellular turnover but also by amino acid uptake, recycling and aminoacyl-tRNA synthesis. To assess the influence of these processes in dynamic SILAC experiments, we have measured the kinetics of isotopic enrichment within intracellular free amino acid and aminoacyl-tRNA precursor pools in dividing and division-arrested neuroblastoma cells following the introduction of extracellular ^{15}N labeled amino acids. We show that the total flux of extracellular amino acids into cells greatly exceeds that of intracellular amino acid recycling and synthesis. Furthermore, in comparison to internal sources, external amino acids are preferentially utilized as substrates for aminoacyl-tRNA precursors for protein synthesis. As a result, in dynamic SILAC experiments conducted in culture, the aminoacyl-tRNA precursor pool is near completely labeled in a few hours and protein turnover is the limiting factor in establishing the labeling kinetics of most proteins.

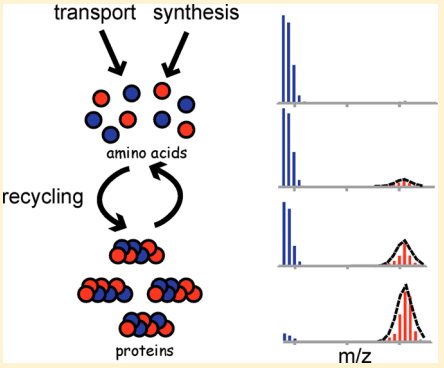

Within cells, proteins are in a state of dynamic equilibrium and are continuously synthesized and degraded.[1,2] Turnover rates are highly variable between proteins and are influenced by their chemical properties (e.g., primary sequence and higher order structure) and the cellular environment within which they are expressed (e.g., organism, tissue, organelle and proteostatic stress).[3−6] Protein turnover plays a critical role in establishing and modulating protein expression levels in numerous normal and pathogenic biological processes and there is great interest in the development of technologies for its quantitative analysis.[7] Historically, quantitative analysis of protein turnover relied on "pulse-chase" analyses and radioactive tracers such as ^{14}C and ^{3}H. More recently, the advent of modern mass spectrometry-based proteomics has opened the door to proteome-wide analyses of protein turnover by utilization of stable isotopes (^{15}N, ^{13}C and ^{2}H).[1] These analyses commonly employ stable isotope labeling in cell culture (SILAC) to quantify the incorporation of isotopically labeled amino acids into proteins as a function time.[8,9] Time-resolved SILAC experiments have made it possible to quantify the degradation kinetics of thousands of proteins without biochemical purification of individual components.

In a typical dynamic SILAC experiment, a single ^{15}N-labeled amino acid is added to the external media and the resulting isotope enrichment within intracellular proteins is measured as a function of time. In such an experiment, the two primary factors that influence the kinetics of protein labeling are the turnover rate of the protein and the relative isotope abundance (RIA) of the aminoacyl-tRNA precursor pool.[1,10] Nonetheless, the latter factor is typically overlooked in SILAC experiments, as it is assumed that the aminoacyl-tRNA precursor pool within the cell becomes fully labeled prior to the turnover of most proteins. However, a number of factors, including slow tracer uptake, amino acid biosynthesis and amino acid recycling, could potentially result in incomplete labeling of the aminoacyl-tRNA precursor pool, especially in early time-points of a SILAC experiment. This issue is of important concern, as incomplete labeling of the precursor pool will result in partial labeling of newly synthesized proteins and significant underestimation of

Received: August 17, 2014
Accepted: October 9, 2014

dx.doi.org/10.1021/ac503067a | Anal. Chem. XXXX, XXX, XXX−XXX

turnover rates in SILAC experiments that utilize a single amino acid probe.

To clarify the potential influence of precursor labeling in dynamic SILAC experiments, we analyzed the kinetics of intracellular free amino acid and aminoacyl-tRNA precursor labeling in neuroblastoma cells following exposure to a fully ^{15}N-labeled media. Given that the proliferative state of the cell is known to greatly influence amino acid transport,[11,12] we conducted our studies in both dividing and division-arrested cells. The labeling of the aminoacyl-tRNA pool at the site of synthesis was quantified at a proteome-wide level by isotopomer analysis[13] of newly synthesized proteins with liquid chromatography tandem mass spectrometry (LC-MS/MS), and the isotopic enrichment of free amino acids in cells were analyzed by gas chromatography mass spectrometry (GC−MS). Together, the results provide important insights into the kinetics of precursor labeling in dynamic SILAC experiments.

EXPERIMENTAL SECTION

Additional experimental details are provided in the Supporting Information.

Cell Growth, Division Arrest, Isotopic Labeling. The Neuro 2a (N2a) neuroblastoma cell line was purchased from American Tissue Culture Collection (CCL131) and cloned by limiting dilution. Cells were initially propagated in Dulbecco's modified Eagle's medium (DMEM) supplemented with 5% fetal bovine serum (FBS). For conducting isotopic labeling in dividing cells, cultures were grown to 30% confluency prior to switching to the labeled media. Cells were collected after 0, 3, 6, 12, 24, 48, 72 and 96 h. To assess the reproducibility of the results, the 0 and 24 h time-points were also obtained in an independent experiment. For conducting isotopic labeling in an arrested state, cells were grown to 80% confluency and treated with 10 mM sodium butyrate. After 2 days of continuous treatment, the media was switched to the labeled media containing 10 mM sodium butyrate. The cells were collected after 0, 3, 6, 12, 24, 48, 74 and 99 h. For all experiments, cells were fed after 2 days with the respective media. Collected cells were washed twice with phosphate buffered saline (PBS) and the numbers of cells were determined with a hemocytometer. Cell pellets were stored in −80 °C for further experiments.

Sample Preparation for LC-MS/MS. A buffer containing 150 mM sodium chloride, 1% sodium deoxycholate, 2% Nonidet P-40 (NP-40) and 2.5% sodium dodecyl sulfate (SDS) was used for cell lysis. Two hundred microliters of lysis buffer was added to approximately 10^6 cells. The samples were sonicated using a high-energy sonicator (Qsonica, Newtown, CT) with 5 s bursts for 30 s (noncontinuous) on ice. The samples were then centrifuged for 30 min at 4 °C at 20000*g*. The middle phases of the samples were transferred to a new tube, while the cell debris pellet and the lipid layer on the surface were avoided. Total protein contents were measured by the bicinchoninic acid assay, and the final protein concentration was adjusted to 1 μg/μL. Protein disulfide bond reduction was carried out in 4 mM Tris(2-carboxyethyl)phosphine at 37 °C for 20 min in an Eppendorf thermomixer, and alkylation was performed with 20 mM iodoacetamine at 37 °C for 30 min in the dark. Proteins were precipitated by a two-step procedure: first, one volume of chilled acetone (at −20 °C) was added so that the mixture turned cloudy but no visible particulate was observed. The mixture was vortexed thoroughly to dissolve the detergents and nonprotein matrix components in the solvent phase. Second, 8 volumes of chilled acetone was added and then incubated at −20 °C overnight. After centrifugation at 4 °C and 20000*g* for 30 min, the supernatant was gently removed and the pellet washed with 800 μL of chilled acetone/water mixture (85/15, v/v %) followed by solvent removal. We then performed a two-step on-pellet-digestion procedure, as previously described.[14−16] Digestion was terminated by adding 1 μL of formic acid followed by centrifugation at 20000*g* for 30 min at 4 °C. The supernatant containing 4 μg of tryptic peptides was injected for each LC-MS/MS analysis.

Nanoflow LC-MS/MS. The Nano-LC system consisted of a Spark Endurance autosampler (Emmen, Holland) and an ultrahigh pressure Eksigent (Dublin, CA) Nano-2D Ultra capillary/Nano-LC system. To achieve a comprehensive and reproducible separation of the complex peptide mixture, a Nano-LC/nanospray setup devised in house[17] was employed. This setup features low void volume, and a large-ID trap column to improve the chromatographic peak shapes, to increase loading capacity, and reproducibility. A long nano-LC column (100 cm long and 75 μm ID, packed with Pepmap 3 μm C18 particles, 100 Å) was employed for extensive separation. To ensure homogeneous and solid packing, the column was packed three times from both ends and then pressurized at 15 000 psi overnight. Quality of packing was confirmed by examination under a microscope. The packed column was "aged" under the gradient conditions (below) for three runs before analysis.

Mobile phases were (A) 0.1% formic acid in 2% acetonitrile and (B) 0.1% formic acid in 88% acetonitrile. Digests containing 4 μg of peptides were loaded onto a large-ID trap (300 μm ID × 5 mm, packed with Zorbax 5 μm C18 material) with 1% B at a flow rate of 10 μL/min, and the trap was washed for 3 min before being brought in line with the nano-LC flow path. A series of nanoflow gradients (the flow rate was 250 nL/min) was used to back-flush the trapped samples onto the nano-LC column for separation. The column was heated at 52 °C in a tightly fitted heating sheath to greatly improve both chromatographic resolution and reproducibility. A 7 h shallow gradient was used to achieve sufficient peptide separation. The optimized gradient profile was as follows: 3 to 8% B over 15 min; 8 to 24% B over 215 min; 24 to 38% B over 115 min; 38 to 63% B over 55 min; 63 to 97% B in 5 min, and finally isocratic at 97% B for 15 min.

An LTQ Orbitrap XL mass spectrometer (Thermo Fisher Scientific, San Jose, CA) was used for detection. The instrument was operating under data-dependent product ion mode. One scan cycle included an MS1 survey scan (m/z 310−2000) at a resolution of 60 000 to acquire precursor peak of peptides, followed by seven MS2 scans at collision-induced dissociation (CID) mode, to fragment the top seven most abundant precursors in the survey scan. The target value for MS1 by Orbitrap was 6×10^6, under which the Orbitrap was calibrated for mass accuracy and FT transmission. The use of high target value on the Orbitrap enabled a highly sensitive detection without compromising the mass accuracy and resolution. The activation time was 30 ms, isolation width was 3 Da for ion trap mass spectrometry (ITMS); the normalized activation energy was 35% and the activation q was 0.25.

Database Search. MS/MS peaklists were extracted using the program PAVA[18] from the LC-MS/MS raw data files corresponding to the unlabeled (t = 0) time-points for both dividing and arrested cells. Peptide identification was conducted by Protein Prospector (version 5.10.12) against the *Mus*

dx.doi.org/10.1021/ac503067a | *Anal. Chem.* XXXX, XXX, XXX−XXX

musculus Uniprot database (downloaded June 17, 2013). To this database, a randomized version was concatenated to allow determination of false discovery rates. The search parameters were the following: species = *Mus musculus*; enzyme specificity = trypsin; allowed missed cleavages = 1; fixed modification = carbmidomethylation; variable modifications = acetylation on protein N terminus, glutamine on peptide N-terminal to glutamic acid, methionine loss from protein N terminus, methionine loss from protein N terminus and acetylation, methionine oxidation; maximal number of variable modifications = 2; parent mass tolerance = 50 ppm; fragment mass tolerance = 0.6 Da; peptide expectation cutoff = 0.05. The match of sequences from the decoy database (normal + random) indicated that the false discovery rates for this expectation cutoff value are 0.16% for arrested cells and 0.14% for dividing cells. A complete list of protein identifications and supporting statistics are provided in the Supporting Information (Excel workbook).

Proteome-wide Determination of ^{15}N Incorporation Ratios and Clearance Rates. Using the Protein Prospector database search results, the following information was gathered for each peptide ion with an expectation value less than 0.05: monoisotopic mass-to-charge ratio (m/z), charge (z), retention time (RT), assigned protein and sequence. The data were tabulated as a text file. Using the program PAVA,[18] MS1 spectra were extracted from all raw data files obtained from the labeling time-course. The MS1 spectra were centroided and the resulting peaklists were used for further analysis. Using a script written in Java (*mssplice*), the following set of analyses were sequentially conducted for each tabulated peptide obtained from the database search: (1) Numbers of nitrogen atoms were determined for each peptide sequence. (2) The possible set of isotopic m/z values for each peptide was determined, assuming a range of 0.0 to 1.0 ^{15}N incorporation ratios. (3) Using a series of overlapping 30 s RT windows, ranging from 2 min prior to 2 min passed the experimentally determined RT, MS1 spectra ranging from the monoisotopic m/z to the maximum possible isotopic m/z (assuming 100% ^{15}N incorporation) were collected and averaged. The total intensity of all possible peptide isotopic m/z values were summed and plotted as a function of RT to generate a chromatogram for each peptide. The chromatogram was fitted with a Gaussian function to determine the peak width. MS1 spectra within the determined RT peak width and the m/z window were summed and the aggregated spectra were used for further analysis. (4) The extracted MS1 peptide spectra were fitted with a probabilistic combinatorial isotopic distribution model that considers the spectra as the sum of two isotopic populations (labeled and unlabeled). The ^{15}N enrichment of the unlabeled population was set as a constant to its natural abundance. The ^{15}N enrichment of the labeled population and the ratio of labeled and unlabeled populations were considered as the two fitted variables. Least-square fitting to the model was used to obtain the following information: the fraction ^{15}N incorporation of the labeled population, the ratio of labeled and unlabeled populations, goodness of fits (coefficient of determination, R^2) to predicted isotopomer distributions for labeled and unlabeled populations. Only spectra that had R^2 values of greater than 0.8 for both populations were used for further analysis. (5) For each peptide ion where more than four unique time-points (t = 0 h and at least three non-zero time-points) passed the above criteria, the fraction labeled values were fitted to a single exponential equation to determine the clearance rate. (6) Peptide level labeled population measurements were aggregated for each homologous group of proteins. Peptides with sequences that were shared among multiple homologous groups were not considered. (7) The aggregated data were fitted with a single exponential equation to determine protein clearance rates. A complete list of measured turnover rates are provided in Supplementary Table 2 (Supporting Information).

GC/MS Analysis of Free Amino Acid Pools. Cultured cells were washed twice with PBS to remove amino acids derived from external media. Protein components of cell lysates (0.5 mg total protein) were precipitated by dilution into cold acetone (800 μL) followed by incubation at −20 °C for 1 h. Free amino acids were isolated from the organic supernatant after evaporation of the solvent under reduced pressure. Dried amino acids were resuspended in 1 mL of 50% acetonitrile, 50 mM K_2HPO_4, pH 11. Pentafluorobenzyl bromide (PFBr, 20 μL) was added, and the sample was sealed and incubated at 100 °C for 1 h. After cooling to room temperature, ethyl acetate (600 μL) was added to each sample followed by mixing. The top layer was then transferred to a fresh tube containing Na_2SO_4. This anhydrous organic solution was injected directly onto a DB-17MS column (30 m × 0.25 mm ID × 0.25 μm film thickness, J&W Scientific, Santa Clara, CA). Analysis was performed on an Agilent 6890N using a chemical ionization (CI) source maintained at 280 °C. Oven temperature was cycled from 140 to 280 °C over a 7.5 min run. Data was collected in SIM mode with a 15 s dwell time using ions corresponding to each amino acid. The enrichment of each amino acid was calculated as described previously.[13] Briefly, the isotopic distribution of ionized fragments from each amino acid was measured at several predetermined time points. Theoretical standard curves describing the isotopic distribution of each amino acid fragment were constructed between the minimum and maximum allowable ^{15}N enrichments. Labeled amino acids in the media represent the maximal possible enrichment at 98.5% ^{15}N. The contribution of the enriched amino acid pool to the spectra was determined using the standard curve. To illustrate an example amino acid analysis, Figure S1 (Supporting Information) outlines the isotopic enrichment quantitation of alanine.

RESULTS AND DISCUSSION

Kinetics of Protein Isotope Labeling in Dividing Cells. We first carried out isotopic labeling experiments in dividing neuroblastoma (N2a) cells. Over the course of 4 days, dividing cells were grown in an isotopically labeled media in which all 20 natural amino acids (the sole source of nitrogen in the media) were ubiquitously labeled with ^{15}N (Figure 1A). It is important to note that this approach differs from typical SILAC experiments where one or a few amino acids (typically lysine and/or arginine) are isotopically labeled. The introduction of the full complement of labeled amino acids enables the determination of the relative isotope abundance (RIA) of the total aminoacyl-tRNA precursor pool by analysis of the mass distribution of newly synthesized proteins (isotopologue distribution). The fractional isotopic labeling within newly synthesized proteins is reflective of precursor RIA at the site of synthesis.[10]

Under the growth conditions utilized in our experiments, the cells had a doubling time of 70 h (Figure S2, Supporting Information). During the course of labeling, the total protein content per cell was at steady-state and remained constant at ~350 pg/cell (Figure S2, Supporting Information). At defined

dx.doi.org/10.1021/ac503067a | *Anal. Chem.* XXXX, XXX, XXX−XXX

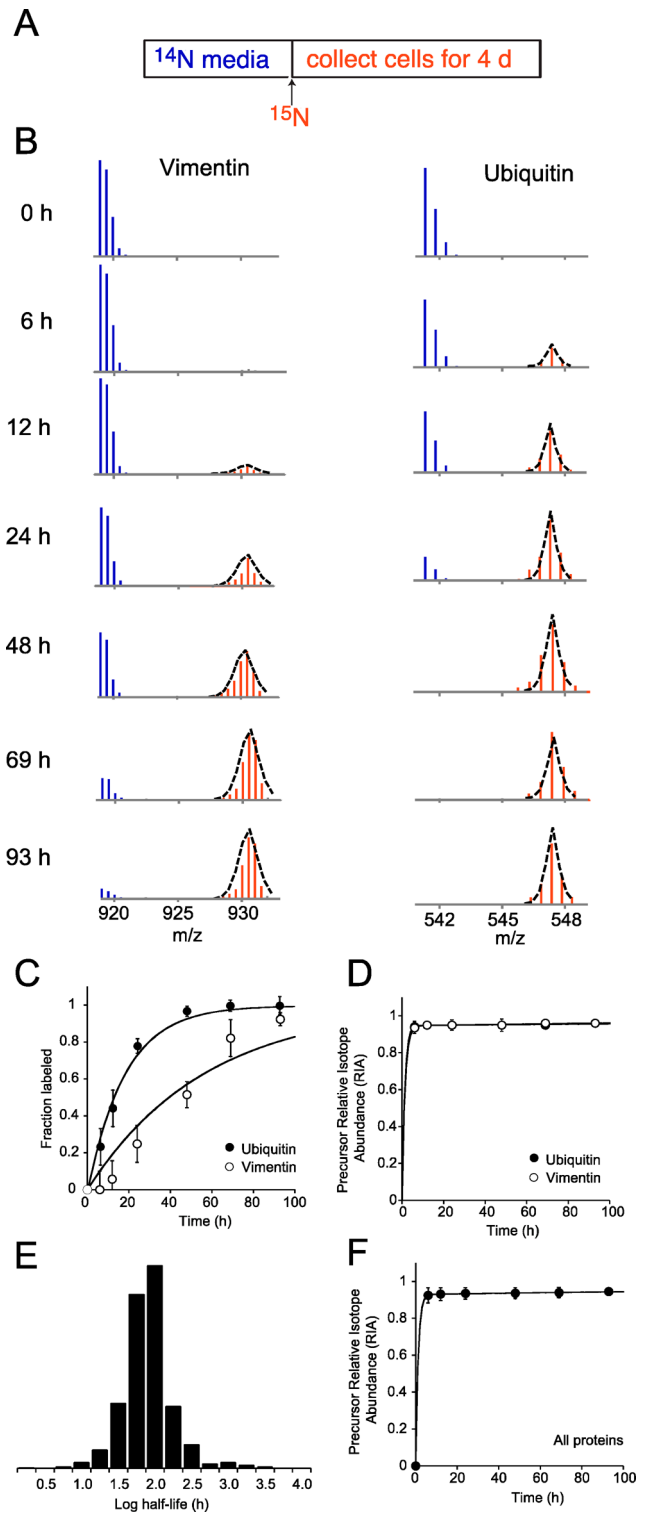

Figure 1. Isotopic labeling of peptides in dividing N2a cells. (A) Experimental design. (B) Mass spectra showing the incorporation of ^{15}N over time in peptides belonging to vimentin (Uniprot P20152, DGQVINETSQHHDDLE, z = 2) and ubiquitin (Uniprot P62983, TLSDYNIQK, z = 2). The blue peaks indicate the chased pool of unlabeled peptides and the red peaks indicate newly synthesized ^{15}N labeled peptides. Each labeled distribution has been fitted with an isotopomer envelope to measure the mass shift and fraction labeled of the labeled population as described in text. (C) Kinetics of fraction labeled and (D) precursor RIA for vimentin and ubiquitin peptides. The points indicate the median values and the error bars indicate the standard deviations for all peptides mapped to the two proteins. For the fraction labeled plot, the lines are fits to a single exponential equation used to determine the clearance rate (k_{clr}). For the precursor RIA plot, the lines are fits to a double exponential equation to account for the two phases of labeling. (E) Distribution of measured protein half-lives in dividing N2a cells determined by subtraction of the cell division rate from k_{clr} values. (F) Global kinetics of precursor relative isotope abundance. The circles indicate the median and the error bars indicate the standard deviation of all measured peptides within the proteome.

time-points following the introduction of ubiquitously ^{15}N labeled media, cell extracts were collected and treated with trypsin using a gel-free digestion protocol.[14] The resulting peptides were analyzed by liquid chromatography tandem mass spectrometry (LC-MS/MS) as described in the Experimental Section. A protein database search was conducted with MS/MS data obtained from unlabeled (time 0) samples. We were able to assign 8475 peptide ions to 1559 nonhomologous proteins (Table 1 and Supplementary Table 1 (Supporting Information)). The false discovery rates, as determined by mock searches against scrambled decoy databases was 0.14%.

Table 1

		dividing	arrested
database search	peptides mapped	8475	9652
	proteins identified	2101	2392
	proteins identified (after homologous filtering)	1559	1783
	decoy hits	3	4
turnover analysis	fraction of identified peptides analyzed	0.37	0.40
	proteins quantified	1159	1534
	mean peptides quantified per protein	6.2	9.9

Retention times (RT) and mass to charge ratios (m/z) of individual unlabeled peptides were used as constraints to extract corresponding regions of MS1 spectra (summed spectra within specific ranges of RT and m/z) for labeled time-points. As examples, Figures 1B shows a series of centroided MS1 spectra corresponding to the labeling time-course of peptides mapped to ubiquitin (a relatively short-lived protein) and vimentin (a relatively long-lived protein). The blue peaks correspond to unlabeled (chased) peptides, and red peaks correspond to labeled newly synthesized peptides. The isotopic distribution of newly synthesized peptides were fitted to a probabilistic combinatorial model[13,19] to determine the fractional incorporation ratio of ^{15}N (see the Experimental Section). This analysis is able to obtain two independent parameters for each MS1 spectra: (1) the fraction of peptides that have shifted in mass following the addition of labeled media (fraction labeled) and (2) the fractional ^{15}N enrichment of newly synthesized proteins. As described above (see the Experimental Section), and by others,[4,10] the former parameter is contingent on the total clearance rate of the protein (k_{clr}) and the latter is equivalent to the isotopic enrichment of the aminoacyl-tRNA precursor pool during synthesis (i.e., precursor relative isotope abundance, RIA). The precision of the measurements was validated by conducting replicate experiments at the 24 h time-point (Figure S3, Supporting Information).

dx.doi.org/10.1021/ac503067a | Anal. Chem. XXXX, XXX, XXX−XXX

For the ubiquitin and vimentin example peptides, the time-dependent change in fraction labeled following the initiation of isotopic labeling is plotted in Figure 1C. The data indicate that the clearance of these peptides occurs in a single exponential phase, which was typical of most peptides in our proteome-wide analysis. For each protein, measurements of fraction labeled for all associated peptides were fitted to a single exponential function to obtain k_{clr} values for each protein (Supplementary Table 2, Supporting Information). On average, the turnover of 6.2 peptides was averaged to determine k_{clr} of a protein. In all, we were able to quantify k_{clr} for 1159 proteins utilizing analysis of three or more time-points for each protein (Table 1, Supplementary Table 2, Supporting Information).

In a dividing cell, the k_{clr} of a protein is established by the sum contribution of its degradation rate (k_{deg}) and the rate of cellular proliferation (the details of the kinetic model are presented in the Supporting Information). We thus determined k_{deg} for all proteins by subtracting the rate of cell division from all protein k_{clr} measurements. The k_{deg} measurements were subsequently converted to half-lives. The global distribution of protein half-life measurements are shown in Figure 1D. Globally, measured protein half-lives ranged from ∼5 to ∼1000 h, with a median value of 58 h. It is interesting to note that the clearance rates of ∼50% of all proteins were less than the rate of cell division (e.g., vimentin shown in Figure 1C), indicating that their observed clearance rate (k_{clr}) was dominated by the diluting effects of cellular proliferation rather than protein degradation.

In contrast to fraction labeled kinetics, the kinetics of precursor RIA were biphasic, with a burst phase that typically reached plateau levels of ∼0.95 followed by a subsequent gradual increases in incorporation ratios (Figure 1D,F). Unlike fraction labeled kinetics, which was highly variable among proteins, the kinetics precursor RIA was largely uniform within the proteome (Figure 1F, error bars). The plateau precursor RIA was reached within the earliest analyzed time-point (6 h). Together, the above data indicate that in dynamic SILAC experiments conducted in a continuously proliferating cell line, the precursor aminoacyl-tRNA pool becomes nearly completely labeled at a rate that exceeds the turnover rate of most detected proteins.

Kinetics of Amino Acid Uptake in Dividing Cells. The rapid and near-complete labeling of the intracellular precursor pool following the introduction labeled amino acids in the external media is somewhat surprising given that amino acid recycling and biosynthetic pathways are expected to contribute significant levels of unlabeled amino acids to the precursor pool during the initial stages of a SILAC experiment. In theory, this outcome may be a result of two independent effects. First, the total flux of external amino acids into cells may exceed the intracellular flux of amino acids due to recycling and biosynthesis. Second, in comparison to intracellularly derived amino acids, transported external amino acids may be preferentially utilized for the formation of charged tRNAs.

To distinguish between these two effects, we independently evaluated the labeling kinetics of intracellular free amino acids. Using the same cell lysates collected during the labeling time-course, proteins were separated from free amino acids by trichloroacetic acid (TCA) precipitation. The free amino acid pool was derivitized with pentafluorobenzyl bromide and analyzed by GC/MS as described in the Experimental Section. Isotopic enrichment of five amino acids (Ala, Gly, Cys, Leu and Phe) was independently measured. This set of amino acids represents a mixture of essential and nonessential amino acids and were the only amino acids that consistently produced sufficiently strong signal intensities on GC/MS to allow for exact quantitation.

The kinetic data indicate that, similar to precursor RIA labeling, the free cellular pools of Ala, Gly, Cys, Leu and Phe become isotopically enriched with biphasic kinetics consisting of a rapid burst within the first few hours followed by a gradual increase over the subsequent 4 days (Figure 2). The biphasic kinetics are consistent with a two-pool model where both transported and internally generated amino acids contribute to the intracellular free amino acids.[20] However, rapidly transported external amino acids appear to be the predominant source of intracellular free amino acids. The relatively smaller contribution of unlabeled amino acids from internal nitrogen stores prevents complete labeling of the free amino acid pool during the initial burst phase. As the cellular protein content is enriched with ^{15}N over time, it gradually recycles labeled amino acids back to the internal pool, resulting in the slow second phase of labeling.

Interestingly, during the course of labeling, free intracellular amino acid RIAs were generally lower than the total aminoacyl-tRNA RIA measured by isotopomer analysis of newly synthesized proteins (Figure 2, dashed lines). This observation suggests that for Ala, Gly, Cys, Leu and Phe, transported extracellular amino acids are preferentially utilized for formation of aminoacyl-tRNAs without complete mixing with the intracellular amino acid pool. Whether this conclusion is valid for other amino acids, including Lys and Arg, which are commonly used probes in SILAC experiments, remains to be determined. However, using a clever double labeling approach, Cambridge et al. have shown that the internal pool of lysines is primarily composed of transported external amino acids rather than amino acids recycled from degradation.[3] Thus, it seems likely that the kinetics of uptake determined for this subset of amino acids is representative of all natural amino acids.

Kinetics of Protein Isotope Labeling in Nondividing Cells. The above data indicate that the rapid influx of external amino acids into cells and their preferential utilization for the formation of aminoacyl tRNAs results in rapid and near complete labeling of the precursor RIA in SILAC experiments within a continuously proliferating cell line. However, non-dividing cells have a lower overall requirement for new protein synthesis and, as a result, have been shown to have slower rates of amino acid uptake.[11,12] To assess the influence of cell division in the kinetics of precursor RIA labeling, we repeated our analyses in division-arrested neuroblastoma cells.

We induced cell division arrest in neuroblastoma (N2a) cells using the sodium salt of *n*-butyric acid (butyrate). In vitro, butyrate is known to block cell replication, inhibit DNA synthesis and promote differentiation in a number of cancer cell lines and stem cells.[21−27] Flow cytometric analysis of cell cycle using a DNA binding dye indicated that butyrate treatment causes cell division arrest by inducing a rapid block in the G1/S transition (Figure S4, Supporting Information).

We carried out isotopic labeling experiments in butyrate-arrested N2a cells. Over the course of 4 days, division arrested cells were maintained in ubiquitously ^{15}N labeled media (Figure 3A). The total protein content per cell was at steady-state during the course of labeling and remained constant at ∼450 pg/cell (Figure S2, Supporting Information). Kinetics of isotope incorporation was analyzed as described above. We were able to assign 9652 peptide ions to 1783 nonhomologous

dx.doi.org/10.1021/ac503067a | *Anal. Chem.* XXXX, XXX, XXX−XXX

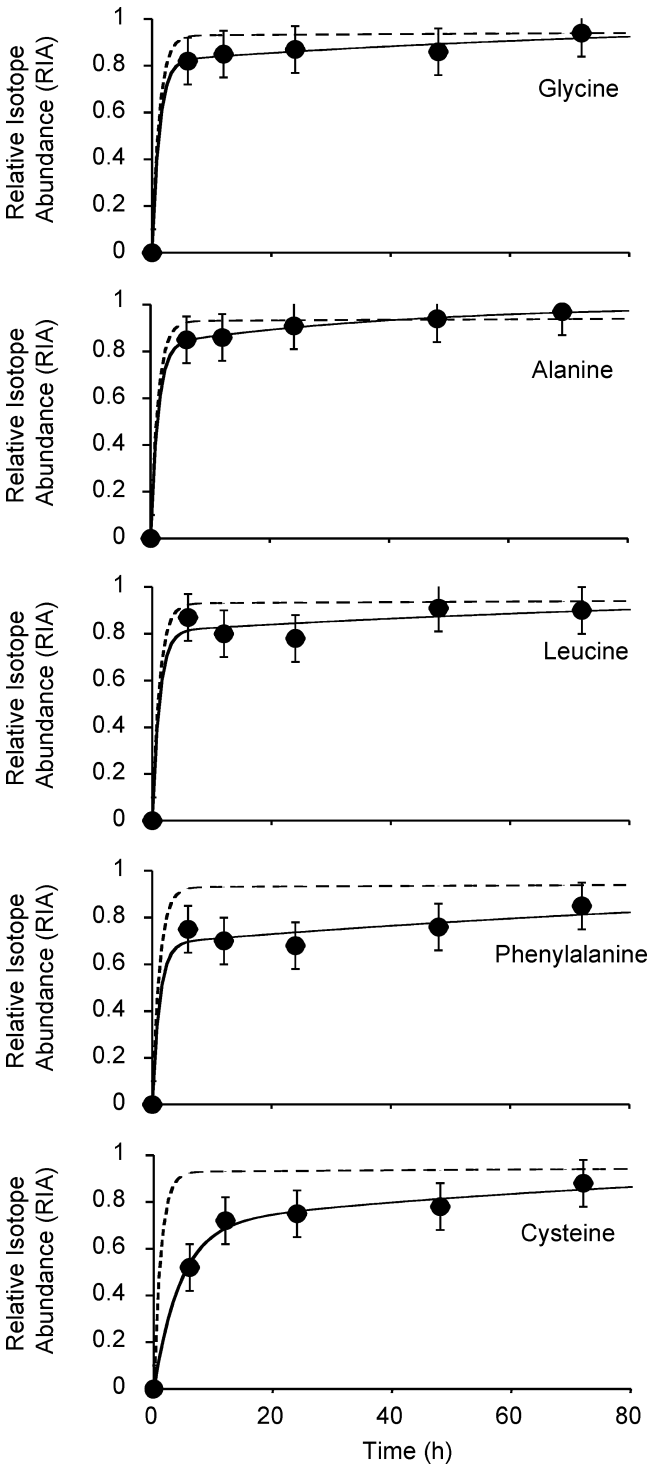

Figure 2. Isotopic labeling of free amino acids in dividing N2a cells. For comparison, the dotted lines indicate the labeling kinetics of the aminoacyl-tRNA precursor relative isotope abundance (Figure 1F).

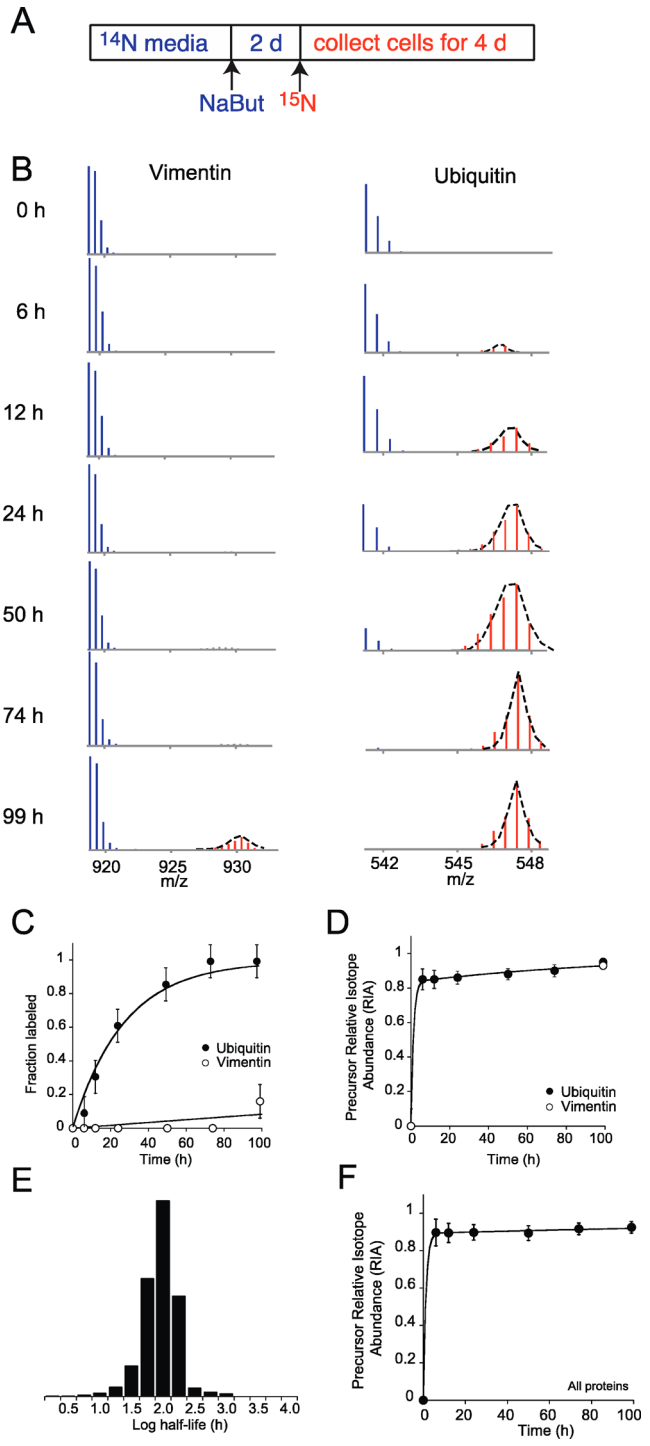

Figure 3. Isotopic labeling of peptides in nondividing N2a cells. Refer to Figure 1 for description of each panel.

proteins (Table 1). Within this set, we were able to quantify k_{clr} for 1534 proteins utilizing analysis of three or more time-points for each protein (Table 1 and Supplementary Table 1, Supporting Information).

In general, the kinetics of fraction labeled for short-lived proteins were similar between dividing and nondividing cells whereas long-lived proteins had a slower rate of clearance (comparison of Figures 1C and 3C and S5, Supporting Information). As has been previously noted,[28] this observation is accounted for by the fact that the contributions of cell division and protein degradation to protein clearance are additive (see the Experimental Section). Whereas protein degradation is the dominant pathway for the clearance of short-lived proteins, long-lived proteins are primarily cleared by the diluting effects of cellular proliferation. As a result, modulation of cell division rates principally influences the clearance kinetics of long-lived proteins. Because the rate of cell division is effectively zero in nondividing cells, protein clearance rates

dx.doi.org/10.1021/ac503067a | Anal. Chem. XXXX, XXX, XXX−XXX

(k_{clr}) determined from fraction labeled kinetics can be used directly to determine protein half-lives (without correcting for the dilution effect of cellular proliferation). Measured protein half-lives in nondividing cells ranged from ~5 to ~1000 h, with a median value of 68 h (Figure 3E).

Labeling of the intracellular aminoacyl-tRNA precursor and free amino acid pools in nondividing cells were analogous to dividing cells. After a few hours, the precursor RIA reached a burst value of ~0.9 and increased gradually in the subsequent 4 days (Figure 3F). The labeling of the precursor pool occurred at a faster rate in comparison to the free intracellular pool of amino acids (Figure 4). Indeed, the discrepancy in labeling kinetics between the amino acyl-tRNA and free amino acids was more pronounced in nondiving cells in comparison to dividing cells. However, although the rate of amino acid transport is decreased in nondividing cells in comparison to dividing cells, the apparent preferential utilization of external amino acids for aminoacyl-tRNA synthesis ensures near complete labeling of the precursor pool within a few hours.

CONCLUSIONS

Time-resolved SILAC experiments have enabled global analyses of protein turnover in a number of cellular systems.[1] In a typical labeling experiment, isotope incorporation in proteins is influenced both by the clearance rate of the protein and the aminoacyl-tRNA precursor RIA. The latter is strongly influenced by the kinetics of tracer uptake, transport, metabolism, catabolism and recycling. When a single amino acid probe is utilized, the kinetics of precursor labeling needs to be taken into account in order to avoid significant underestimations of protein turnover rates. In this study, we have quantitatively analyzed the labeling kinetics of intracellular free amino acid and aminoacyl-tRNA pools following the introduction of isotopically labeled media to a dividing and stationary neuroblastoma cell line. The results allow us to assess the potential influence of precursor labeling on the kinetics of protein labeling in dynamic SILAC experiments.

Our results indicate that in both dividing and stationary cells, amino acid uptake is rapid and the free amino acid pool inside the cell is isotopically enriched within a few hours after the introduction of labeled media. Interestingly, the magnitude of ^{15}N enrichment at a given time-point is generally lower for free amino acid pools in comparison to the aminoacyl-tRNA pool (and thus synthesized polypeptides). This observation is consistent with a number of historical radiotracer studies indicating that extracellular amino acids can be direct precursors for protein synthesis without complete mixing with the intracellular amino acid pool.[29−34] It has been suggested that this phenomenon may be caused by the specific localization of aminoacyl-tRNA synthetases on or near the plasma membrane such that their catalytic activity is coupled to amino acid transport.[35−37]

Together, our results indicate that the rapid and complete labeling of the aminoacyl-tRNA pool in SILAC experiments is accounted for by two related phenomena. First, the total flux of extracellular amino acids into cells exceeds that of intracellular amino acid recycling and synthesis. Second, in comparison to internal sources, external amino acids are preferentially utilized as substrates for aminoacyl-tRNA precursors for protein synthesis. As a result, in dynamic SILAC experiments conducted in culture, it is protein turnover, and not precursor labeling, that is the dominant factor in establishing the labeling kinetics of proteins whose half-life exceeds a few hours. For analysis of proteins with shorter half-lives, strategies may need to be employed to deconvolute the kinetics of protein turnover from precursor labeling. For these proteins, the utilization of multiple labeled amino acid probes and isotopomer analysis provides a powerful approach for quantifying precursor labeling at the site of synthesis. This approach is also critical in analysis of protein turnover in complex organisms where label uptake into tissues has been shown to be slow relative to rates of turnover for many proteins.[4]

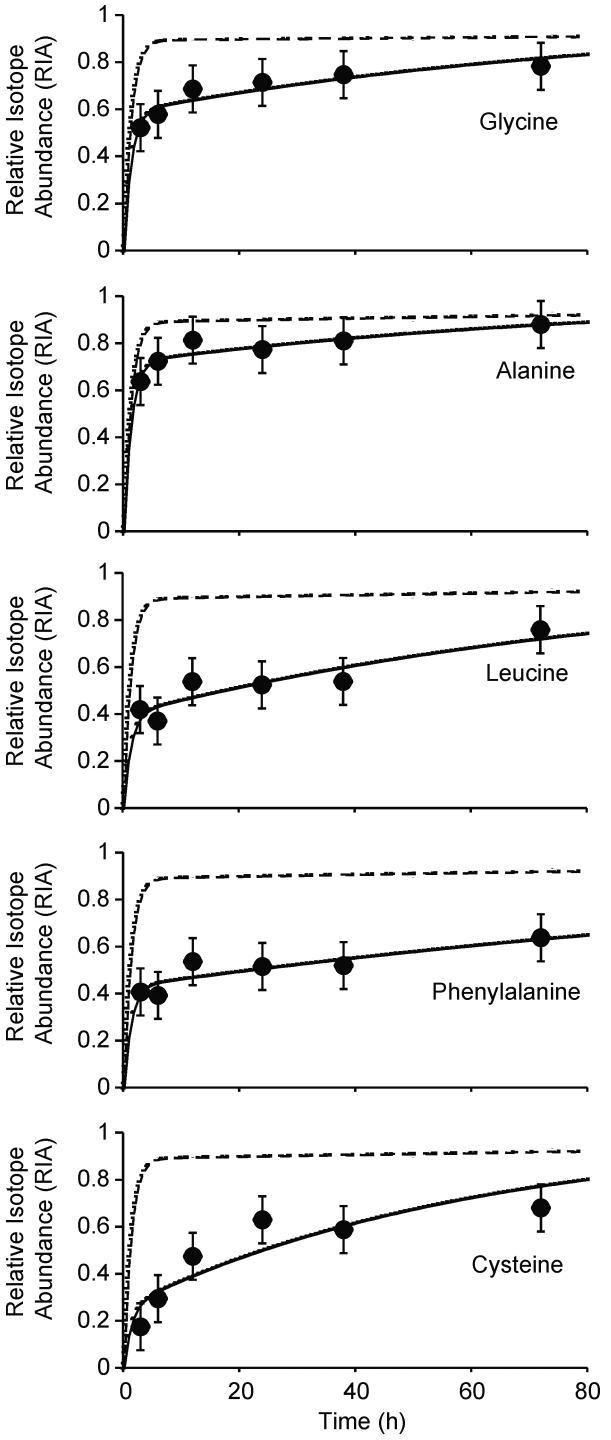

Figure 4. Isotopic labeling of free amino acids in nondividing N2a cells. For comparison, the dotted lines indicate the labeling kinetics of the aminoacyl-tRNA precursor relative isotope abundance (Figure 3F).

dx.doi.org/10.1021/ac503067a | Anal. Chem. XXXX, XXX, XXX−XXX

■ ASSOCIATED CONTENT

Supporting Information

Additional information as noted in text. This material is available free of charge via the Internet at http://pubs.acs.org.

■ AUTHOR INFORMATION

Corresponding Author

*S. Ghaemmaghami. Address: Department of Biology, University of Rochester, 326 Hutchison Hall, Rochester NY 14627. Tel: (585) 275-4829. Fax: (585) 275-2070. E-mail: sghaemma@bio.rochester.edu.

Notes

The authors declare no competing financial interest.

■ ACKNOWLEDGMENTS

We thank Timothy Riiff, and Joan Protasio at KineMed Inc. for their expertise and assistance in collecting the gas chromatography data and Olga Dunaevsky for assistance in cell culture.

■ REFERENCES

(1) Claydon, A. J.; Beynon, R. *Mol. Cell. Proteomics* **2012**, *11*, 1551−1565.
(2) Schoenheimer, R. *The Dynamic State of Body Constituents*; Harvard University Press: Boston, 1942.
(3) Cambridge, S. B.; Gnad, F.; Nguyen, C.; Bermejo, J. L.; Kruger, M.; Mann, M. *J. Proteome Res.* **2011**, *10*, 5275−5284.
(4) Price, J. C.; Guan, S.; Burlingame, A.; Prusiner, S. B.; Ghaemmaghami, S. *Proc. Natl. Acad. Sci. U. S. A.* **2010**, *107*, 14508−14513.
(5) Schwanhausser, B.; Busse, D.; Li, N.; Dittmar, G.; Schuchhardt, J.; Wolf, J.; Chen, W.; Selbach, M. *Nature* **2011**, *473*, 337−342.
(6) Toyama, B. H.; Savas, J. N.; Park, S. K.; Harris, M. S.; Ingolia, N. T.; Yates, J. R., 3rd; Hetzer, M. W. *Cell* **2013**, *154*, 971−982.
(7) Hinkson, I. V.; Elias, J. E. *Trends Cell Biol.* **2011**, *21*, 293−303.
(8) Mann, M. *Nat. Rev. Mol. Cell Biol.* **2006**, *7*, 952−958.
(9) Ong, S. E.; Blagoev, B.; Kratchmarova, I.; Kristensen, D. B.; Steen, H.; Pandey, A.; Mann, M. *Mol. Cell. Proteomics* **2002**, *1*, 376−386.
(10) Doherty, M. K.; Whitehead, C.; McCormack, H.; Gaskell, S. J.; Beynon, R. J. *Proteomics* **2005**, *5*, 522−533.
(11) Guidotti, G. G.; Borghetti, A. F.; Gazzola, G. C. *Biochim. Biophys. Acta* **1978**, *515*, 329−366.
(12) Oxender, D. L.; Lee, M.; Cecchini, G. *J. Biol. Chem.* **1977**, *252*, 2680−2683.
(13) Hellerstein, M. K.; Neese, R. A. *Am. J. Physiol.* **1992**, *263*, E988−1001.
(14) Duan, X.; Young, R.; Straubinger, R. M.; Page, B.; Cao, J.; Wang, H.; Yu, H.; Canty, J. M.; Qu, J. *J. Proteome Res.* **2009**, *8*, 2838−2850.
(15) Tu, C.; Li, J.; Bu, Y.; Hangauer, D.; Qu, J. *J. Proteomics* **2012**, *77*, 187−201.
(16) Tu, C.; Li, J.; Young, R.; Page, B. J.; Engler, F.; Halfon, M. S.; Canty, J. M., Jr.; Qu, J. *Anal. Chem.* **2011**, *83*, 4802−4813.
(17) Tu, C.; Li, J.; Jiang, X.; Sheflin, L. G.; Pfeffer, B. A.; Behringer, M.; Fliesler, S. J.; Qu, J. *Mol. Cell. Proteomics* **2013**, *12*, 3583−3598.
(18) Guan, S.; Price, J. C.; Prusiner, S. B.; Ghaemmaghami, S.; Burlingame, A. L. *Mol. Cell. Proteomics* **2011**, *10*, M111.010728.
(19) Rockwood, A. L.; Van Orden, S. L. *Anal. Chem.* **1996**, *68*, 2027−2030.
(20) Guan, S.; Price, J. C.; Ghaemmaghami, S.; Prusiner, S. B.; Burlingame, A. L. *Anal. Chem.* **2012**, *84*, 4014−4021.
(21) Terao, Y.; Nishida, J.; Horiuchi, S.; Rong, F.; Ueoka, Y.; Matsuda, T.; Kato, H.; Furugen, Y.; Yoshida, K.; Kato, K.; Wake, N. *Int. J. Cancer* **2001**, *94*, 257−267.
(22) Rodriguez-Paredes, M.; Esteller, M. *Nat. Med. (N. Y., NY, U. S.)* **2011**, *17*, 330−339.
(23) Andriamihaja, M.; Chaumontet, C.; Tome, D.; Blachier, F. *J. Cell. Physiol.* **2009**, *218*, 58−65.
(24) Crea, F.; Nobili, S.; Paolicchi, E.; Perrone, G.; Napoli, C.; Landini, I.; Danesi, R.; Mini, E. *Drug Resist. Updates* **2011**, *14*, 280−296.
(25) Rawluszko, A. A.; Slawek, S.; Gollogly, A.; Szkudelska, K.; Jagodzinski, P. P. *Biomed. Pharmacother.* **2012**, *66*, 77−82.
(26) Mohamed Ariff, I.; Mitra, A.; Basu, A. *J. Neurosci. Res.* **2012**, *90*, 529−539.
(27) Mali, P.; Cheng, L. *Stem Cells* **2012**, *30*, 75−81.
(28) Eden, E.; Geva-Zatorsky, N.; Issaeva, I.; Cohen, A.; Dekel, E.; Danon, T.; Cohen, L.; Mayo, A.; Alon, U. *Science* **2011**, *331*, 764−768.
(29) Van Venrooij, W. J.; Poort, C.; Kramer, M. F.; Jansen, M. T. *Eur. J. Biochem.* **1972**, *30*, 427−433.
(30) Airhart, J.; Vidrich, A.; Khairallah, E. A. *Biochem. J.* **1974**, *140*, 539−545.
(31) Hod, Y.; Hershko, A. *J. Biol. Chem.* **1976**, *251*, 4458−4457.
(32) Reith, M. E.; Schotman, P.; van Zwieten, B. J.; Gispen, W. H. *J. Neurochem.* **1979**, *32*, 413−420.
(33) Robertson, J. H.; Wheatley, D. N. *Biochem. J.* **1979**, *178*, 699−709.
(34) Gehrke, L.; Ilan, J. *Proc. Natl. Acad. Sci. U. S. A.* **1983**, *80*, 3274−3278.
(35) Van Venrooij, W. J.; Moonen, H.; Van Loon-Klaassen, L. *Eur. J. Biochem.* **1974**, *50*, 297−304.
(36) Moore, P. A.; Jayme, D. W.; Oxender, D. L. *J. Biol. Chem.* **1977**, *252*, 7427−7430.
(37) Shotwell, M. A.; Mattes, P. M.; Jayme, D. W.; Oxender, D. L. *J. Biol. Chem.* **1982**, *257*, 2974−2980.